Astronomische Gesellschaft: Reviews in Modern Astronomy **14**, 209–222 (2001)

The FORS Deep Field

Jochen Heidt[1], Immo Appenzeller[1], Ralf Bender[2], Asmus Böhm[3], Nive Drory[2], Klaus J. Fricke[3], Achim Gabasch[2], Ulrich Hopp[2], Klaus Jäger[3], Martin Kümmel[4], Dörte Mehlert[1], Claus Möllenhoff[1], Alan Moorwoord[5], Harald Nicklas[3], Stefan Noll[1], Roberto Saglia[2], Walter Seifert[1], Stella Seitz[2], Otmar Stahl[1], Eckhard Sutorius[1], Thomas Szeifert[1,6], Stefan J. Wagner[1], Bodo Ziegler[3]

[1] Landessternwarte Heidelberg, Königstuhl, 69117 Heidelberg, Germany
[2] Universitätssternwarte München, Scheinerstraße 1, 81679 München, Germany
[3] Universitätssternwarte Göttingen,
Geismarlandstraße 11, 37083 Göttingen, Germany
[4] Max-Planck-Institut für Astronomie, Königstuhl 17, 69117 Heidelberg, Germany
[5] European Southern Observatory,
Karl-Schwarzschild-Straße 2, 85748 Garching, Germany
[6] European Southern Observatory Santiago,
Alonso de Cordova 3107, Santiago 19, Chile

Abstract

Dedicating a major fraction of its guaranteed time, the FORS consortium established a FORS Deep Field which contains a known QSO at $z = 3.36$. It was imaged in UBgRIz with FORS at the VLT as well as in J and Ks with the NTT. Covering an area 6–8 times larger as the HDFs but with similar depth in the optical it is one of the largest deep fields up to date to investigate i) galaxy evolution in the field from present up to $z \sim 5$, ii) the galaxy distribution in the line of sight to the QSO, iii) the high-z QSO environment and iv) the galaxy-galaxy lensing signal in such a large field. In this presentation a status report of the FORS Deep Field project is given. In particular, the field selection, the imaging results (number counts, photometric redshifts etc.) and the first spectroscopic results are presented.

1 Introduction

Deep fields are one of the most powerful tools to explore galaxy evolution over a wide redshift range. The main aim of this kind of studies is to constrain evolutionary scenario such as the hierarchical structure formation typical of Cold Dark Matter universes (e. g. Kauffmann 1996) or the picture of monolithic collapse, which assumes galaxy formation at very high redshifts and passive

evolution (e. g. Larson 1974). Those studies are typically performed in several subsequent steps. Images with the best possible resolution, as deep and covering an area as large as possible, are used to study the morphology of the objects of interest. A combination of several optical and near-IR broad-band (and in some cases narrow-band) images of a deep field allow to estimate photometric redshifts, which in turn can be used to either preselect (classes of) objects for follow-up spectroscopy or even constrain galaxy evolution without spectroscopical confirmation for objects beyond the reach of current 8–10 m class telescopes. Finally, spectroscopy of individual (classes of) galaxies are used to derive their kinematics and to investigate their chemical composition, star formation histories etc.

The Hubble Deep Field North (HDF-N, Williams et al. 1996) and related follow-up observations e. g. with Keck dramatically improved our knowledge of galaxy evolution in the redshift range $z = 1$–4. It is the deepest view of the sky ever made, with excellent resolution, but it has only a relatively small field of view ($\sim$ 5.6 sq. arcmin). In contrast, the Calar Alto Deep Imaging Survey (CADIS, Meisenheimer et al. 1998) is less deep, but covers a much larger area (several 100 sq. arcmin) and searches specifically for primeval galaxies in the redshift range $z = 4.6$–6.7. By now, several other Deep Field studies have been conducted or are underway, such as the NTT Deep Field (Arnouts et al. 1999), the WHT Deep Field (McCracken et al. 2000) or the DEEP Survey (see e. g. Koo 1999). All these Deep Fields fall inbetween the HDF-N and CADIS in terms of deepness, resolution and area surveyed.

The FORS instruments for the VLT1 and VLT2 telescopes have been built by a consortium of the State Observatory in Heidelberg, the University Observatory in Göttingen and the University Observatory in Munic (Appenzeller et al. 1992). For their efforts the three institutes received guaranteed observing time on the 2 VLT telescopes with the FORS instruments. In order to use the guaranteed time efficiently, it was decided to spent a major fraction of the guaranteed time in establishing a FORS Deep Field (FDF). The advantages are obvious. The FDF conducted on a 8 m class telescope allows imaging nearly as deep as is possible for the HDFs, with lower resolution, but a 6–8 times larger field of view (providing better statistics) and efficient follow-up multi-object spectroscopy with the same instruments. Moreover, it provides a large pool of data for projects carried out within the three institutes involved, which are supported financially by the government including two SFBs (SFB 439 "Galaxies in the young universe" in Heidelberg, SFB 375 "Astro particle physics" in Munic), and the VW foundation programme ("Kinematic evolution of galaxies" in Göttingen).

In this article, a status report of the FDF project as of September 2000 is presented. In the following, the field selection will be described, and the scientific aspects which will be addressed, will be summarized. Then, the results from the imaging part will be presented, followed by a short overview of the photometric redshifts. Finally, first spectroscopical results are shown and one of the scientific highlights so far briefly discussed. The very first observations (selection of the FDF) started almost 2 years ago, whereas the

imaging part has been conducted in Fall 1999. Since the annual meeting of the Astronomische Gesellschaft 2000 in Bremen, the major part of the follow-up spectroscopy was also completed. This subject, however, will only be touched briefly.

2 Field selection

A critical aspect for a project such as the FDF is the selection of a suitable field. Owing to various constraints, the following selection criteria were adopted:

1) The field should be free of astronomical objects brighter than 19th mag (to avoid saturation during periods of excellent seeing conditions, to avoid reflexes on the CCD and minimize overhead for readout, slewing etc.).

2) It should not contain any (known) galaxy cluster (to avoid a distorsion of galaxy number counts).

3) The field should have good observability (close to zenith at Paranal).

4) In order to go as deep as possible and to allow observations in other wavebands low galactic extinction, low H I column density and low IR-cirrus is required.

5) Strong x-ray sources and radio sources in the field should be avoided (to exclude potential galaxy clusters at high redshift).

6) No bright stars (< 5 mag) within 5° should be present (to avoid possible reflexes and straylight from the telescope structure).

7) A (radio-quiet) QSO at redshift > 3 should be present in the field (to study QSO environment at high z and the IGM along the line of sight to the QSO).

Due to the items 1, 4 and 6 the south galactic pole was a good region on the sky to start. Therefore all the QSO neighborhoods, which fulfilled criteria 3 and 7 close to the south galactic pole (and thus favouring criteria 1, 4 and 6) were selected from the QSO catalogue of Véron-Cetty & Véron (7. edition, 1997). This resulted in 32 candidates. Afterwards an extensive search in the literature and catalogs from radio up to x-ray bands, a visual check of the DSS and photometry provided by the COSMOS scans was carried out, which revealed 4 promising candidates. These 4 candidates were observed during the commissioning phase of FORS1, which showed that 3 of them were not useful (they either contained relatively bright galaxy clusters or had problems with the observability due to the absence of suitable guide stars at the VLT). Finally, a field with the center coordinates $\alpha_{2000} = 01^{\rm h}06^{\rm m}03.6^{\rm s}$, $\delta_{2000} = -25°45'46''$ containing the QSO Q 0103–260

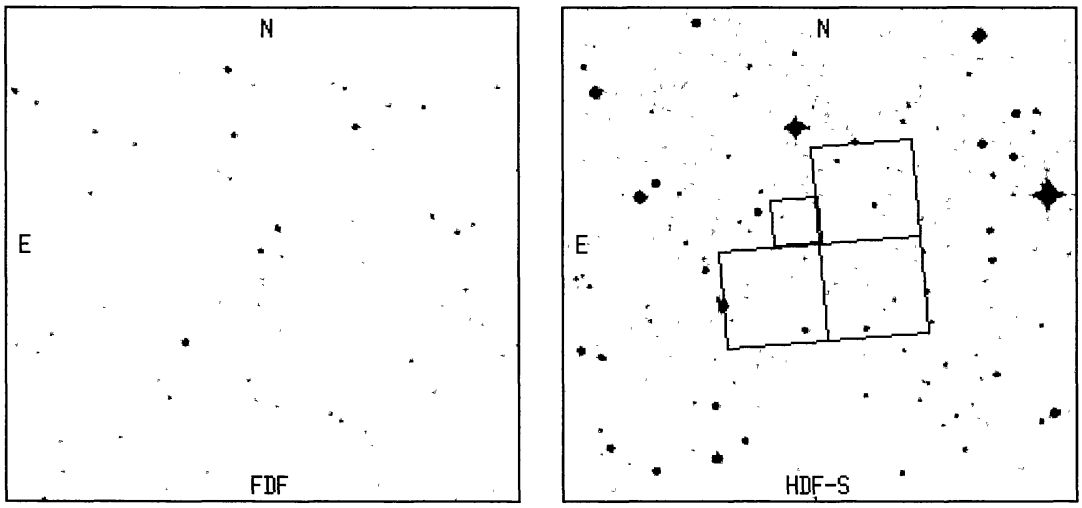

Figure 1: DSS plots of the FDF and of a field of the same size surrounding the HDF-S. Note the much lower surface density of bright foreground objects and the absence of bright stars in the FDF region.

($z = 3.36$) was chosen as the FDF. The DSS print in Figure 1 shows a comparison of the FDF and the HDF-S.

3 Projects within the FDF

The main aim of the FDF is to study the galaxy evolution in the redshift range between $z = 1$–5 (morphology, chemical abundances, star formation rates, number counts etc.). More specific projects address the evolution of the Tully-Fisher relation in field spirals between $z = 0.2$–1 and the evolution of field ellipticals between $z = 0.2$–0.6. Additionally, the QSO host and its environment (cluster properties and L_α-galaxies) as well as absorption line systems along the line of sight to the QSO will be studied. Finally, galaxy-galaxy lensing signals and QSO statistics will be investigated.

4 Observations

The imaging of the FDF was carried out mainly with FORS1 during 5 runs between August and December 1999. During those runs, observations in UBgRIz and two narrow band filters (530_25 and 485_37, the former centered at Lyα at the QSO's redshift, to search for Lyα-galaxies around $z = 3.36$) were taken. During periods of unfavourable seeing (which unfortunately occurred several times) multi-object spectroscopy of ~ 120 galaxy candidates in the FDF was made. The galaxy candidates were selected from preliminary photometric redshifts based on optical data of the FDF taken during the field selection procedure.

Images of the FDF in J and Ks were acquired with the NIR camera SOFI at the NTT in October 1999. The main purpose of the NIR images was to optimize the photometric redshifts for follow-up spectroscopy. The majority of the multi-object spectroscopic observations of high-redshift galaxy candidates was carried in two runs within three weeks after the annual meeting of the Astronomische Gesellschaft 2000 in Bremen. During these runs excellent spectra of ~ 230 galaxy candidates with photometric redshifts mainly between $z = 1$–5 (and a few $z = 6$ candidates) could be collected.

5 Results

5.1 Imaging

An overview about the imaging results for each individual filter (as of September 2000) along with the total integration time, the PSF FWHM of the summed image, the field of view (FOV) and $5\,\sigma$ completeness limits for galaxies are presented in Table 1. The FOVs of the individual optical filters differ somewhat, which is caused by few positioning errors of the telescope and/or the fact that the images have been taken in different runs. While the total integration times are within our expectations, the completeness limits are not. This mainly due a relatively low efficiency of the telescope and the CCD (resulting in a loss of approx. 0.4 mag) at the time of the observations. Moreover, the seeing was on average more worse than expected. Still, we detected $\sim 10^4$ galaxies in the FDF. For example, we detected ~ 6500 galaxies in B band ($\sim$ 4100 up to B = 27.75), ~ 8600 galaxies in R band ($\sim$ 5100 up to R = 26.75) and ~ 7500 galaxies in I band ($\sim$ 4600 galaxies up to I = 26.25). The total integration time in J and Ks was relatively low, which is due to the relatively

Table 1 Overview about the imaging observations.

Filter	Time [hours]	FWHM [″]	FOV [′]	Completeness (5 σ) [mag]
U	10.7	1.15	6.2 × 6.4	25.50
B	4.4	0.95	5.8 × 5.8	27.50
g	5.0	1.00	6.3 × 6.4	27.00
R	5.8	0.85	6.4 × 6.4	26.75
I	4.0	0.60	6.1 × 5.8	26.25
z	3.5	0.75	6.8 × 6.8	?
530_25	4.0	0.80	6.8 × 6.8	?
485_37	3.0	0.85	6.8 × 6.8	?
J	1.7	0.80	6.8 × 7.9	22.50
K	1.7	0.75	6.8 × 7.9	20.50

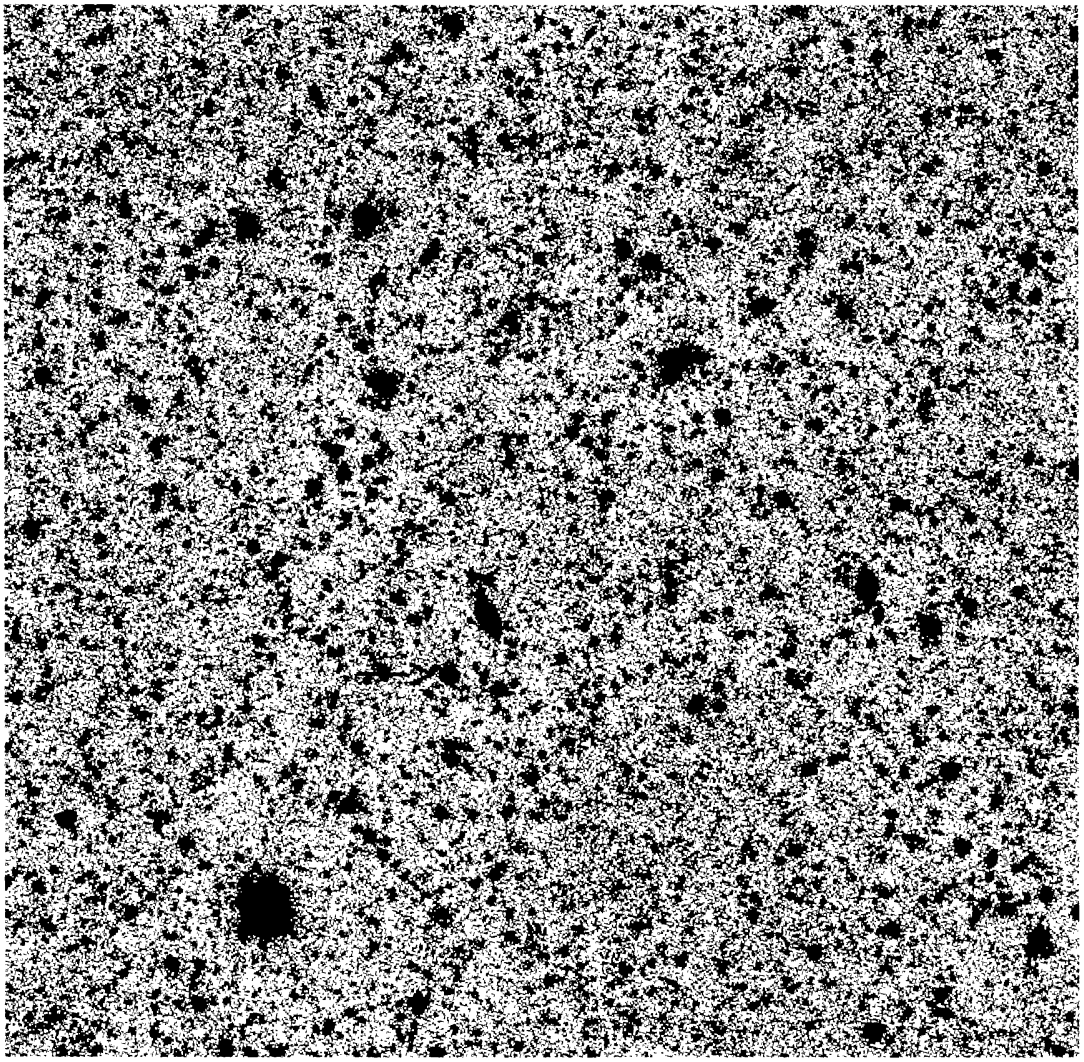

Figure 2: The FDF in B band from FORS observations. This frame contains $\sim$ 6500 galaxies. Integration time is 4.4 h, FWHM $= 0.95''$, FOV $= 5.8' \times 5.8'$. North is up, east to the left. The QSO is marked with an arrow.

small FOV of SOFI as compared to FORS. Therefore a mosaic of four pointings was necessary. Since the SOFI subfields had some overlap, some parts of the FDF (including the QSO) were exposed much longer (up to 6.8 h).

In Figure 2, the FDF in B band is shown. Obviously, the galaxies are homogeneously distributed in the FDF. The brightest object is an elliptical galaxy in the lower southeastern part of the FDF with B $\sim$ 18.5. Unfortunately, there is still a (fortunately not very rich) galaxy cluster at $z \sim 0.3$ in the southwestern corner of the FDF.

The "quality" of the FDF can also be demonstrated by the galaxy number counts. As an example, the galaxy number counts in B band for the FDF are compared to those derived by Metcalfe et al. 1995 (WHT/INT observations), Williams et al. 1996 (HDF-N), Arnouts et al. 1999 (NTT Deep Field) and

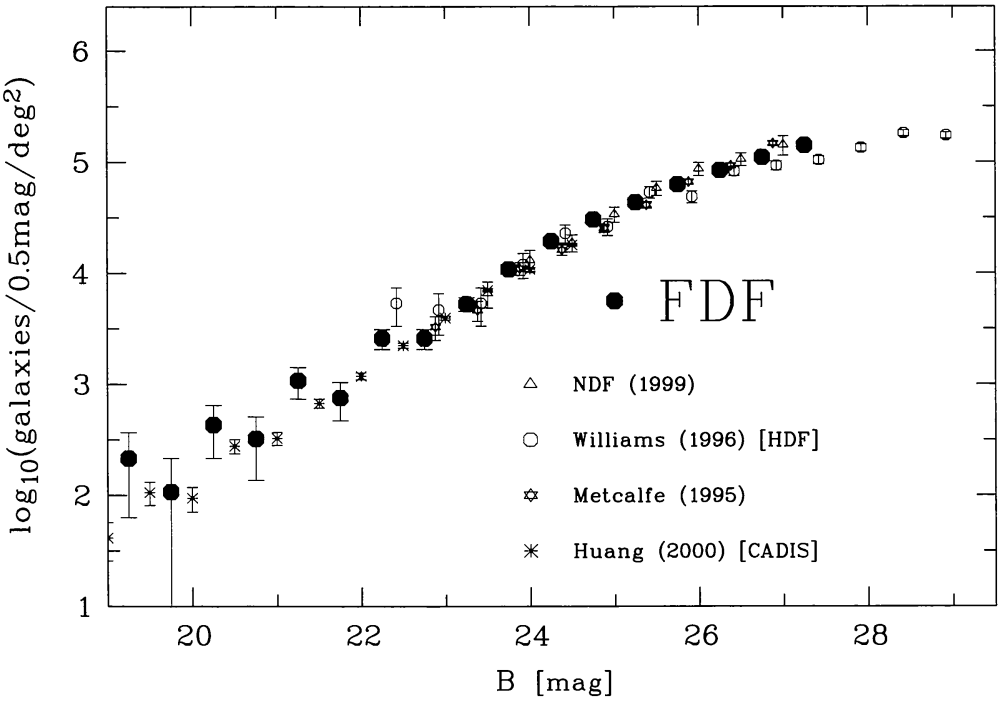

Figure 3: Galaxy number counts of the FDF in B band as compared to other deep surveys.

Huang et al. 2000 (CADIS). In general there is an excellent agreement over almost 9 mag, with some scatter at the bright end. This might be due to the contamination of the galaxy cluster in the southeastern corner of the FDF, which is still small.

It is also tempting to compare the completeness limits of the FDF to those of other Deep Fields. These are shown for the broad-band optical filters in Table 2 in comparison to the HDF-N and the NTT Deep Field. Whereas the FDF is $\sim$ 0.5–1 mag deeper as the NTT Deep Field, it is 0.4–1.3 mag less deep as the HDF-N. Given the loss of 0.4 mag due to the low efficiency of the VLT and the CCD, the FDF is indeed comparable to the HDF-N except in the I filter. This is no surprise, however, since atmospheric effects (airglow) does not effect the space-borne HST. It should be noted that the FOV of the FDF is a factor of 6 larger ($\sim$ 36 sq. arcmin) as compared to the HDF-N and the NTT Deep Field ($\sim$ 5.6 sq. arcmin). Finally, it should be emphasized that the integration times are comparable to the NTT Deep Field, whereas the HDF-N was exposed between 4 and 8 times longer.

Table 2 Limiting magnitudes of the FDF compared to those of the NTT Deep Field and the HDF-N.

	FDF			NTT DF			HDF-N	
	lim 5 σ	FWHM ["]	Time [hours]	lim 5 σ	FWHM ["]	Time [hours]	lim 10 σ	Time [hours]
U	25.50	1.15	10.7				27.0	43
B	27.50	0.95	4.4	26.9	0.90	14.7	27.9	33.5
g	27.00	1.00	5.0	26.5	0.83	6.5	28.0	30
R	26.75	0.85	5.8	25.9	0.83	6.5		
I	26.25	0.60	4.0	25.3	0.70	4.5	27.6	34

5.2 Photometric redshifts

Photometric redshifts were estimated by fitting template spectra of different galaxy types/stars and varying redshift to the measured fluxes on the optical and NIR images of the objects (see Bender 2001 for details). In order to minimize biases (e. g. by absorption through dust) an I-band selected sample was chosen. Photometric redshifts and object types could be estimated for $\sim$ 3800 objects. Most objects of the I-band selected sample are Im/Irr-type galaxies, about 15 % are early (E/S0) or late-type (Sa/Sb/Sc) galaxies, about 5 % (190) are most likely stars. The major fraction of the galaxies have photometric redshifts between $z = 0$ and 3, a few objects have photometric redshifts between $z = 5$ and 6 (some, perhaps all of which might be late-type M or L stars). In general, the early-type galaxies haver lower redshifts than the late-type galaxies, which have a similar redshift distribution as the Im/Irr-galaxies. This is illustrated in Figure 4, where the distribution of the full galaxy sample and two subsamples are shown. For comparison, fits to the photometric redshift distribution of the HDF-S and HDF-N are shown as well. In general, the distributions of the photometric redshifts between the FDF and the two HDFs are quite similar. The reliability of the photometric redshifts can be tested best by a comparison to spectroscopic redshifts from real data. This was possible, since spectra of $\sim$ 120 galaxy candidates could be collected already during the imaging part of the FDF (see above). A comparison is presented in Figure 5. As can be seen, there is a very good consistency between the photometric and spectroscopic redshifts (the former having errors of typically $\leq$ 10 %), with only a few outliers. Hence, the photometric redshifts are an excellent preselection criteria for follow-up spectroscopy the I-band selected galaxy sample.

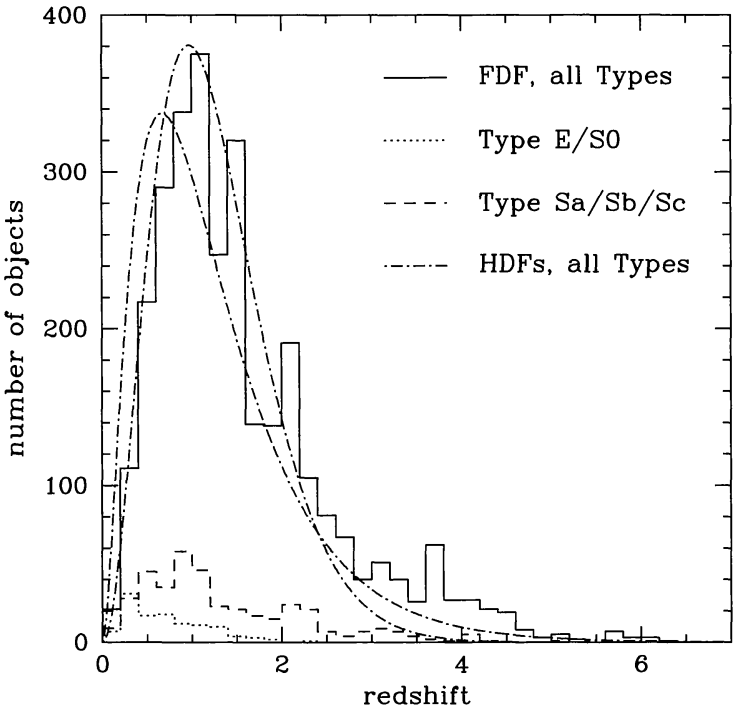

Figure 4: Distribution of the photometric redshifts estimated from an I-band selected sample (3600 galaxies) in the FDF. The dotted line represents the early-type galaxies, the dashed line the late-type galaxies and the solid line the sum of all galaxy types (early-type, late-type and Im/Irr). For comparison fits to the distributions of photometric redshifts from the HDFs are shown.

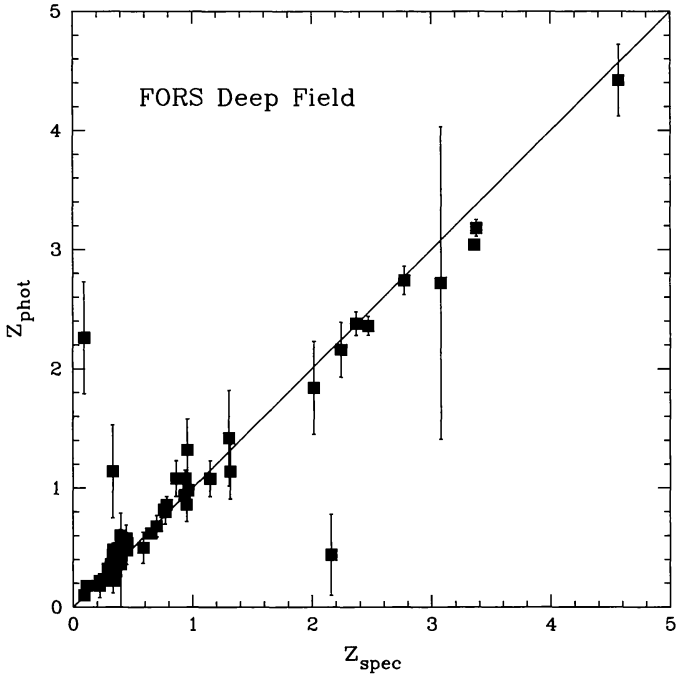

Figure 5: Comparison of spectroscopic and photometric redshifts for $\sim$ 100 galaxies in the FDF. Note the very good agreement for almost all galaxies.

5.3 Spectroscopy

During the imaging part of the FDF spectra of $\sim$ 120 (relatively bright) galaxy candidates could be collected. Most of the objects (65) turned out to be galaxies at low redshift ($z < 1$), stars (20) or unidentified objects (20). Nevertheless, also 15 galaxies with $z = 1$–4 were found, thus illustrating the power of the VLT even under relatively poor observing conditions. The spectrum of a $z = 2.773$ galaxy from those observations is shown in Figure 6. This galaxy is dominated by a strong (rest frame) UV continuum, has no strong emission lines, but many high ionisation metallic lines in absorption indicating strong starburst activity. For illustration we display the appearance of this galaxy in B, R, I and K on the same figure. On the B-band frame the galaxy is clearly visible with some hint of an elongation towards the south, which is more prominent in the R-band image. A nearby galaxy (early-type, photometric redshift $\sim$ 0.36) to the southeast can also be seen. On the I-band image, the southern extension is somewhat separated from the $z = 2.773$ galaxy. Moreover, due to the good seeing of that image, an extension towards the northeast become visible. Although the K-band image is not very deep, the three components ($z = 2.773$ galaxy, companion at $z_{\rm phot} = 0.36$ and southern extension) are present as well. Although this is a bit speculative, the starbursting $z = 2.773$ galaxy might be in interaction with either extension to the south or north or in some merger stage. This has frequently been observed in galaxies at high redshift.

5.4 Environment of QSO Q0103–260 ($z = 3.36$)

While broad-band imaging of the FDF was mainly carried out for determining photometric redshifts (target selection for spectroscopic follow-up) and morphological studies, narrow-band imaging was conducted specifically to search for Lyα-galaxies at the QSOs redshift. The first results from the latter are encouraging. In Figure 7 the environment of the QSO in the narrow-band image centered at the redshifted Lyα of the QSO (530_25) are compared to the image taken with another narrow-band filter (485_37) and the broad-band I image. On the broad-band I image the photometric redshifts of individual galaxies are displayed.

Several interesting features can bee seen on that Figure. On the 530_25 filter image two objects a few arcsec southeast and southwest of the QSO are detected, which are not visible on the 485_37 filter image, but faintly present on the broad-band I image. Moreover, one of the two objects has a photometric redshift ($z = 3.08$), close to the QSOs redshift. Additionally, an object with a similar photometric redshift ($z = 3.06$) was found, which is a few arcsec to the northwest of the QSO. Given an error of $\leq 10\,\%$ for photometric redshifts of such faint objects (mainly due to the errors of the photometry) the QSO might well be surrounded by a group of at least 3 galaxies, two of which having relatively strong Lyα-emission. Alternatively, the three galaxies (or at least some of them) might be along the line of sight to the QSO, thus

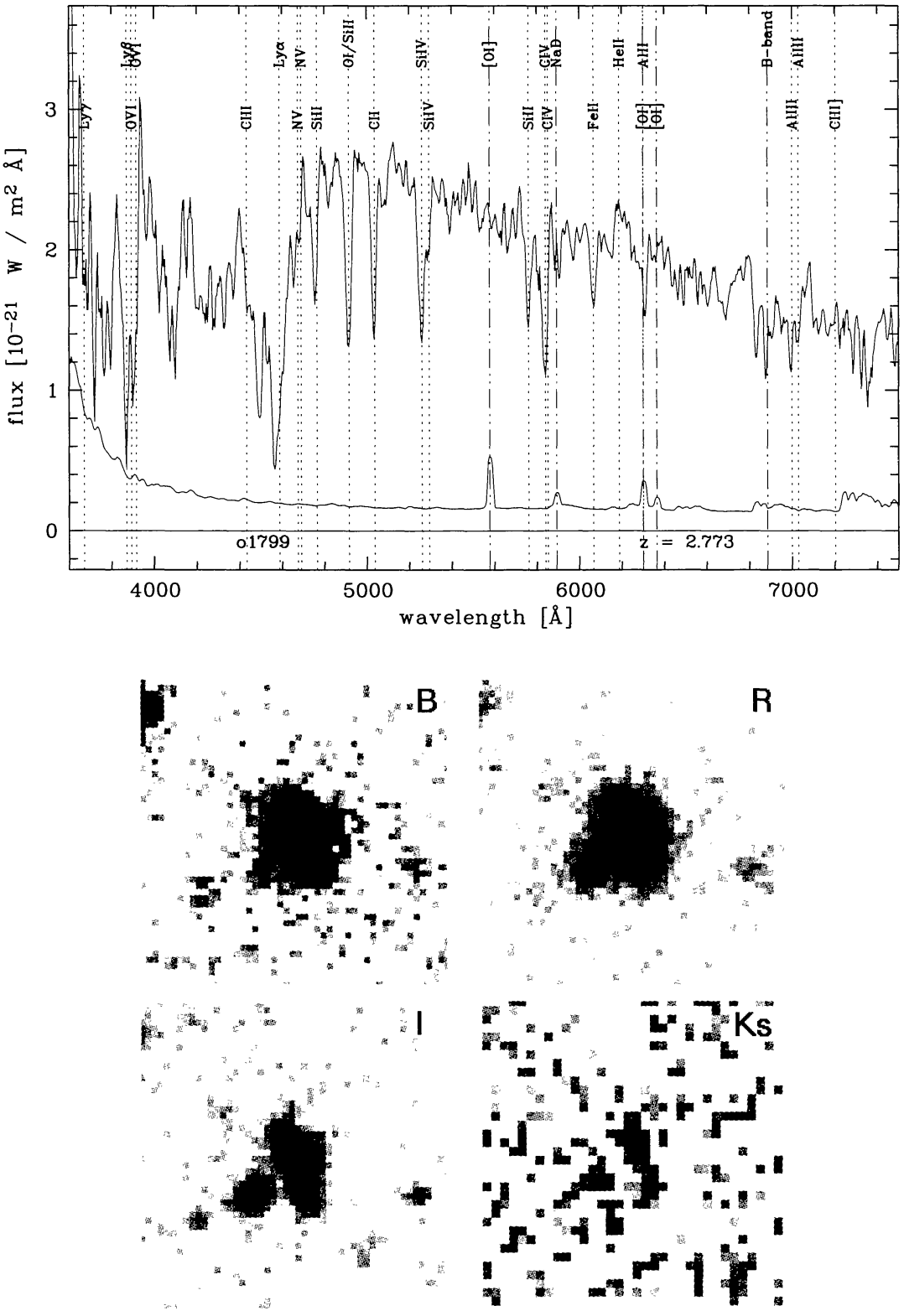

Figure 6: Top: Spectrum of a $z = 2.773$ FDF galaxy. Note the strong UV (rest frame) continuum and the absence of strong emission lines. Bottom: Images of the $z = 2.773$ galaxy in B, R, I and Ks. North is up, east to the left. FOV is $10'' \times 10''$. See text for details.

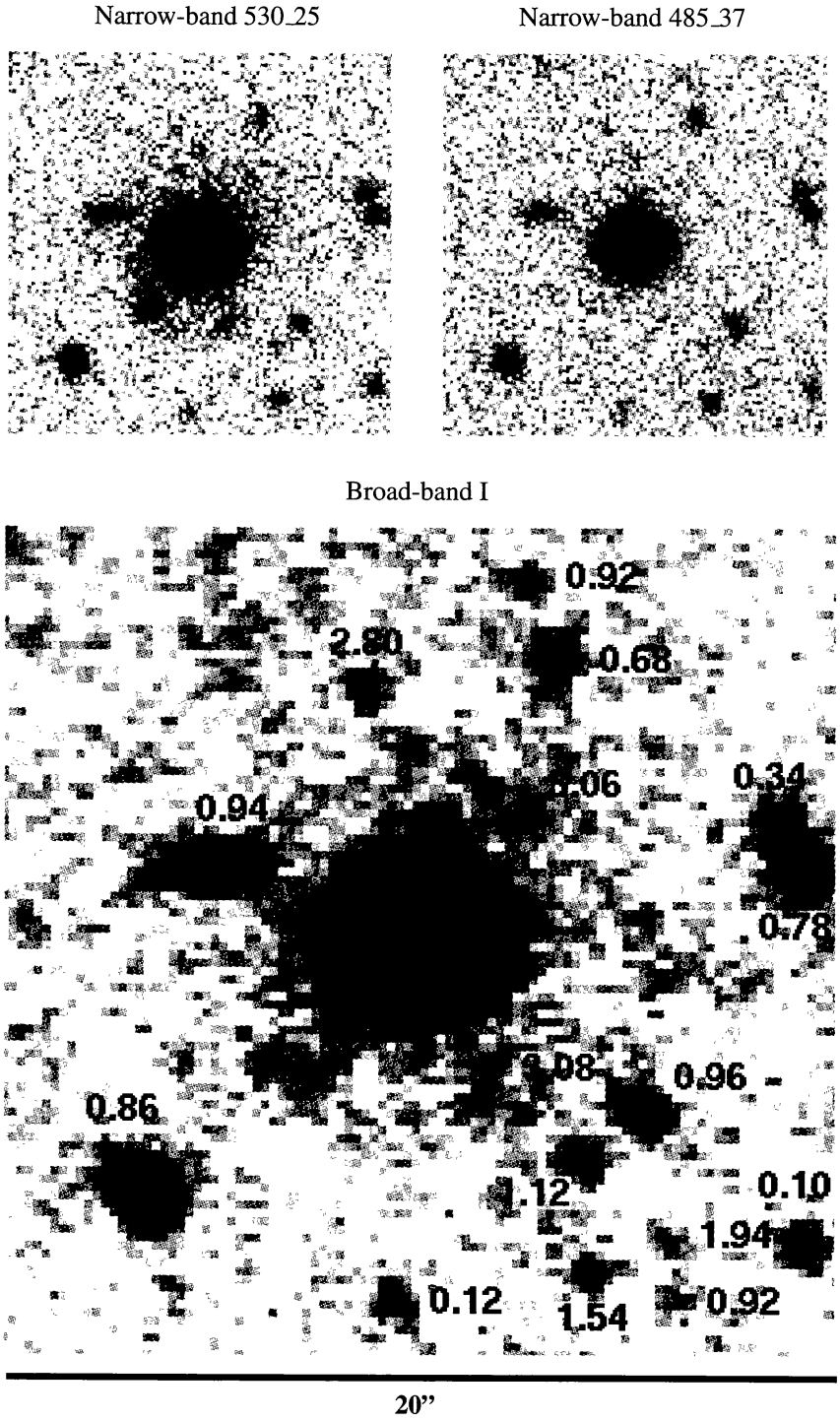

Figure 7: Narrow-band image of the QSO environment centered at the redshifted Lyα of the QSO (530_25, top left) compared to the second narrow-band image (485_37, top right) and the broad-band I image (bottom). Note the two objects a few arcsec southeast and southwest of the QSO on the 530_25 image, which are not visible on the 485_37 image. A further object at photometric $z = 3.06$ is present on the broad-band I image. These three sources may form a small group with the QSO or are along the line-of-sight to the QSO.

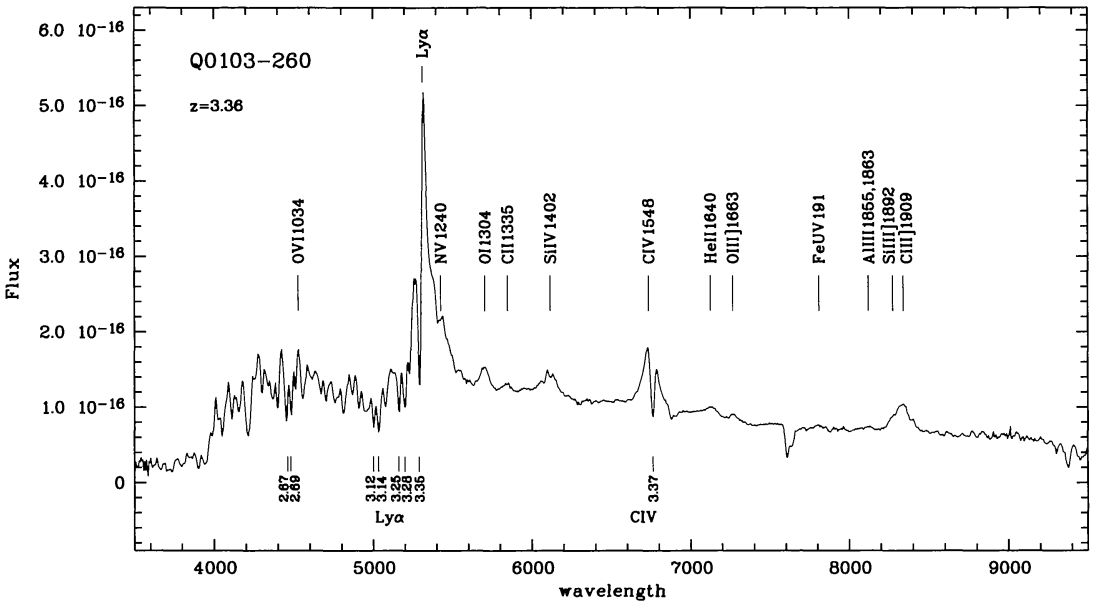

Figure 8: Low-resolution spectrum of QSO Q0103–260 at $z = 3.36$. Several prominent emission lines typical for QSOs as well as a few absorption absorption lines and their corresponding redshifts are marked.

being responsible for absorption-line systems in the spectrum of the QSO. Indeed, some absorption-line systems close to $z = 3.36$ have been detected in a low-resolution spectrum of the QSO (Figure 8).

Spectroscopy of these three sources with FORS at the VLT will clarify the possible physical association with the QSO. Since the sources are relatively faint ($m_I = 25$) this is a challenging task even for an 8m class telescope. Finally, a high-resolution spectrum of the QSO with UVES at the VLT will allow the identification of the absorption-line systems more accurately. Joined together, the nature and physics of these objects can then be studied in detail.

6 Summary and outlook

The first observations of the FDF started a bit more than one year ago. During that time, the imaging part was carried out. The analysis of the data (photometric redshifts, galaxy number counts etc.) is essentially completed. Although the observing conditions (seeing) were not as good as anticipated and although some light was lost due to the lower efficiency of the telescope (degrading CCD etc.) the FDF is one of the deepest view of a region on the sky ever made from ground, nearly comparable as the HDFs, but with a factor of 6 larger area surveyed. Spectra of approximately 120 objects in the FDF were collected as well, which were primarily used to prove the reliability and to optimize the photometric redshift code. Some of these spectra are also useful for the main aim of the FDF – the study of the evolution of galaxies at early epochs. The first analysis of the narrow-band images is encouraging. Three objects, presumably galaxies, nearby the QSO could be identified, which are

either physically associated with the QSO, or are along the line-of-sight to the QSO thus responsible for the absorption line systems in the QSO spectrum.

Since the annual meeting of the Astronomische Gesellschaft in autumn 2000 in Bremen, the major part of the spectroscopical observations was carried out. Spectra for more than 200 high-z galaxy candidates could be taken with FORS at the VLT. The preliminary results confirm the reliability of the photometric redshift code further. This will allow to study the properties of the high-z galaxies statistically, which are unobservable spectroscopically due to their faintness even with the VLT. On the other hand, the high-quality spectra for more than 200 galaxies in the redshift range $z = 1$–5 (with the current highest-z galaxy at a redshift of $z \sim 4.6$ (S. Noll, priv. com.)) form an excellent database for future investigations of the evolution of galaxies in the early universe.

Acknowledgments

It is a pleasure to thank the organizers of the annual meeting of the Astronomische Gesellschaft 2000 in Bremen for the opportunity to present the FORS Deep Field project. The generous support by the Paranal and La Silla staff during the various observing runs is gratefully acknowledged. This work was supported by the Deutsche Forschungsgemeinschaft (SFB 375, SFB 439), the VW foundation and the German Federal Ministry of Science and Technology with ID-Nos. 05 2HD50A, 05 2GO20A and 05 2MU104.

References

Appenzeller I., Rupprecht G. et al., 1992, Messenger 67, p. 18

Arnouts S., D'Odorico S., Cristiani S. et al., 1999, A&A 341, 641

Bender R., 2001, The FORS Deep Field: Photometric redshifts and object classification, Workshop on Deep Fields, in press

Huang J. S., Thompson D. J., Kümmel M. W. et al., 2000, A&A submitted

Kauffmann G., 1996, MNRAS 281, 487

Koo D., 2000, Exploring distant galaxy evolution: Highlights with Keck. In: Reviews in Modern Astronomy 13 (R. E. Schielicke, ed.), p. 173

Larson R. B., 1974, MNRAS 166, 585

McCracken H. J., Metcalfe N., Shanks T. et al., 2000, MNRAS 311, 707

Meisenheimer K., Beckwith S., Fockenbrock R. et al., 1998, The Calar Alto Deep Imaging Survey (CADIS). In: The young universe: galaxy formation and evolution at intermediate and high redshift (S. O'Dorico, A. Fontana, E. Giallongo, eds.), ASP Conf. Ser. 136, p. 134

Metcalfe N., Shanks T., Fong R., Roche N., 1995, MNRAS 273, 257

Véron-Cetty M.P., Véron P., 1997, A catalogue of Quasars and Active Nuclei (7. edition)

Williams R. E., Blacker B., Dickinson M. et al., 1996, AJ 112(4), 1335